International Journal of Solids and Structures 49 (2012) 2778–2792

Contents lists available at SciVerse ScienceDirect

International Journal of Solids and Structures

journal homepage: www.elsevier.com/locate/ijsolstr

Homogenization of thick periodic plates: Application of the Bending-Gradient plate theory to a folded core sandwich panel

A. Lebée, K. Sab *

Université Paris-Est, Laboratoire Navier (École des Ponts ParisTech, IFSTTAR, CNRS), École des Ponts ParisTech, 6 et 8 avenue Blaise Pascal, 77455 Marne-la-Vallée cedex 2, France

ARTICLE INFO

Article history:
Available online 3 January 2012

Keywords:
Plate theory
Higher-order models
Sandwich panels
Homogenization
Periodic plates
Folded cores
Chevron pattern

ABSTRACT

In a previous paper from the authors, the bounds from Kelsey et al. (1958) were applied to a sandwich panel including a folded core in order to estimate its shear forces stiffness (Lebée and Sab, 2010b). The main outcome was the large discrepancy of the bounds. Recently, Lebée and Sab (2011a) suggested a new plate theory for thick plates – the Bending-Gradient plate theory – which is the extension to heterogeneous plates of the well-known Reissner–Mindlin theory. In the present work, we provide the Bending-Gradient homogenization scheme and apply it to a sandwich panel including the chevron pattern. It turns out that the shear forces stiffness of the sandwich panel is strongly influenced by a skin distortion phenomenon which cannot be neglected in conventional design. Detailed analysis of this effect is provided.

1. Introduction

Sandwich panels are widespread in everyday life. Their structural efficiency is well-known and is a main criterion in possible applications. They are made of a light and thick core which is glued between two stiff skins. When the sandwich panel is bent, the skins are put into traction and compression. Thus, their design consists in maximizing their mechanical properties. This is not the case of the core which role in the sandwich panel is to resist shear forces. It must be as light as possible but not too weak. Hence the design of a core is driven by a trade-off between lightness and mechanical properties. This trade-off led to a wide diversity of cores in which cellular materials take a center stage. Among them, honeycomb structures are still considered as the most efficient cellular core geometries in many respect for high performance sandwich panels in aeronautics. However, they have some drawbacks. The iterative production process makes it an expensive material. Furthermore, once glued between skins, their cells are closed which makes them prone to store water condensation during successive take-off and landing of airplanes. This water damages the bound between core and skin and caused unexpected delaminations. Thus core design is still an innovative field nowadays. In order to tackle these drawbacks, folded cores gained new interest from the industry because of new production means and an open cell geometry.

Folded core patterns are really ancient and emerged mostly from the art of folding paper (Origami) and pleating techniques for textile (see Atelier Lognon, Paris, for instance). Therefore, the use of a periodic folded pattern as a core is well-known since the emergence of sandwich panel technology and some patents date back to the first use of honeycomb cores (Hochfeld, 1959; Rapp, 1960; Gewiss, 1960). However they remained largely ignored because of the lack of an efficient production process. Recently, continuous production means were developed (Basily and Elsayed, 2004a; Basily and Elsayed, 2007; Kehrle, 2004) which might create a new market for this type of core.

This regain of interest led to several studies concerning folded cores. Pattern generation was studied in details (Kling, 1997, 2005) and led to a broad variety of configurations. The present work is dedicated to the chevron pattern (Fig. 1) which is the simplest pattern and one of the first to be used as a core in sandwich panels. A large amount of experimental work was done in order to investigate the mechanical behavior of these cores. Basily and Elsayed (2004b), Nguyen et al. (2005) and Heimbs et al. (2010) mostly studied impacts on sandwich panel including folded cores. Kintscher et al. (2007) loaded folded cores with both transverse shear and compression up to failure. Fischer et al. (2009) and Baranger et al. (2010a) focused on the behavior of the aramid paper used in folded cores. Moreover, in order to spare experimental burden, intensive numerical simulations were performed by Heimbs (2009), Fischer et al. (2009) and Baranger et al. (in press). The final objective is to implement "virtual testing" tools. These works point out the influence of the knowledge of the constitutive material as

* Corresponding author. Tel.: +33 1 64153749; fax: +33 1 64153741.
E-mail addresses: arthur.lebee@enpc.fr (A. Lebée), karam.sab@enpc.fr (K. Sab).

0020-7683/$ - see front matter © 2011 Elsevier Ltd. All rights reserved.
doi:10.1016/j.ijsolstr.2011.12.009

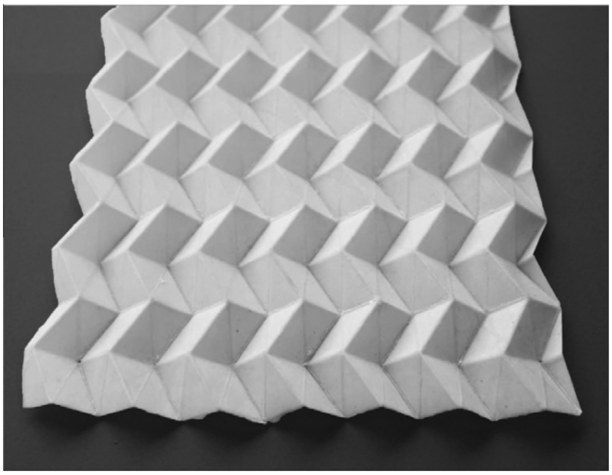

Fig. 1. Chevron folded paper.

well as the critical influence of the geometrical defects on the strength of folded cores. However the core is always separated from the skins in these studies, which precludes any possible interaction between skins and core.

As already mentioned, the main action of the core is to carry shear forces. Thus, the first mechanical property one wants to assess is the shear forces stiffness of the sandwich panel and then, even more critically, the strength of the sandwich panel under shear forces. Actually, very few methods exist for such estimation because the behavior of thick plates is still a theoretical issue. The main reason is the ignorance of the effect of shear forces at microscopic scale (the unit-cell in the case of periodic sandwich panels). However, when dealing with sandwich panels, it is generally acknowledged that the skins simply put the core into transverse shear. Based on this argument, Kelsey et al. (1958) suggested bounds for estimating shear forces stiffness of sandwich panels including honeycomb. Basically, they apply uniform shear stress or strain directly to the core alone, replacing the action of the skins. In the case of chevron pattern, the upper bound was first derived by Miura (1972). Then Lebée and Sab (2010b) derived both upper and lower bounds and demonstrated that with manufactured geometries, they were very loose (more than 100% discrepancy). This gap between bounds comes from the omission of possible interaction between the skins and the core. Usually, engineers refer to the upper bound, implicitly assuming that the skins remain very stiff (Kelsey et al., 1958). However, sandwich panel theory relies on the assumption of thin skins which is an antagonistic demand. Thus we need more refined homogenization techniques in order to compute exactly the shear forces stiffness. A new theory for thick plates with varying constitutive material through the thickness was suggested in Lebée (2010) and Lebée and Sab (2011a). This theory, called Bending-Gradient theory, makes very few assumptions on the plate configuration and was successfully applied to highly anisotropic laminated plates under cylindrical bending with various material configurations (Lebée and Sab, 2011b).

The aim of this paper is to apply this new plate theory to a sandwich panel including the chevron pattern. It is organized as follows. First, in Section 2, the Bending-Gradient plate theory is summarized and the related homogenization scheme is provided. Then the sandwich panel including chevron pattern is introduced and details about implementation are given in Section 3. Results and validation with a full 3D simulation are presented in Section 4. Finally, we bring out the interaction between skins and core. The relevant parameters are identified and their influence in sandwich panel design is discussed in Section 5.

2. The Bending-Gradient plate model and its homogenization scheme

In this section, we first introduce the main features of the notations used in this article. Then the Bending-Gradient plate theory is summarized. Finally the extension to periodic plates is performed using energy equivalence.

2.1. Notations

Vectors and higher-order tensors are boldfaced and different underlinings are used for each order: vectors are underlined, $\underline{\boldsymbol{u}}$. Second order tensors are underlined with a tilde: $\underset{\sim}{\boldsymbol{M}}$ and $\underset{\sim}{\boldsymbol{e}}$. Third order tensors are underlined with a parenthesis: $\underset{\frown}{\boldsymbol{\Phi}}$ and $\underset{\frown}{\boldsymbol{\Gamma}}$. Fourth order tensors are doubly underlined with a tilde: $\underset{\approx}{\boldsymbol{D}}$ and $\underset{\approx}{\boldsymbol{c}}$. Sixth order tensors are doubly underlined with a parenthesis: $\boldsymbol{F}$ and $\boldsymbol{I}$.

When dealing with plates, both 2-dimensional (2D) and 3D tensors are used. Thus, $\hat{\underline{\boldsymbol{T}}}$ denotes a 3D vector and $\underline{\boldsymbol{T}}$ denotes a 2D vector or the in-plane part of $\hat{\underline{\boldsymbol{T}}}$. The same notation is used for higher-order tensors: $\hat{\underset{\sim}{\boldsymbol{\sigma}}}$ is the 3D second-order stress tensor while $\underset{\sim}{\boldsymbol{\sigma}}$ is its in-plane part. When dealing with tensor components, the indexes specify the dimension: a_{ij} denotes the 3D tensor $\hat{\underset{\sim}{\boldsymbol{a}}}$ with Latin index $i, j, k,.. = 1, 2, 3$ and $a_{\alpha\beta}$ denotes the 2D tensor $\underset{\sim}{\boldsymbol{a}}$ with Greek indexes $\alpha, \beta, \gamma,.. = 1, 2$.

The transpose operation ${}^{t}\cdot$ is applied to any order tensors as follows: $({}^{t}A)_{\alpha\beta\ldots\psi\omega} = A_{\omega\psi\ldots\beta\alpha}$. Three contraction products are defined, the usual dot product ($\hat{\underline{\boldsymbol{a}}} \cdot \hat{\underline{\boldsymbol{b}}} = a_i b_i$), the double contraction product ($\hat{\underset{\sim}{\boldsymbol{a}}} : \hat{\underset{\sim}{\boldsymbol{b}}} = a_{ij} b_{ji}$) and a triple contraction product ($\underset{\frown}{\boldsymbol{A}} \therefore \underset{\frown}{\boldsymbol{B}} = A_{\alpha\beta\gamma} B_{\gamma\beta\alpha}$). Einstein's notation on repeated indexes is used in these definitions. The derivation operator $\hat{\underline{\boldsymbol{\nabla}}}$ is also formally represented as a vector: $\hat{\underset{\sim}{\boldsymbol{a}}} \cdot \hat{\underline{\boldsymbol{\nabla}}} = a_{ij} \nabla_j = a_{ij,j}$ is the 3D divergence and $\underset{\sim}{\boldsymbol{a}} \otimes \underline{\boldsymbol{\nabla}} = a_{\alpha\beta} \nabla_\gamma = a_{\alpha\beta,\gamma}$ is the 2D gradient. Here $\otimes$ is the dyadic product.

2.2. Summary of the Bending-Gradient model (macro scale)

We consider a linear elastic plate which mid-plane is the 2D domain $\omega \subset \mathbb{R}^2$. Cartesian coordinates (x_1, x_2, x_3) in the reference frame $(\hat{\underline{\boldsymbol{e}}}_1, \hat{\underline{\boldsymbol{e}}}_2, \hat{\underline{\boldsymbol{e}}}_3)$ are used to describe macroscopic fields. The plate is loaded exclusively with the out-of-plane distributed force $\hat{\underline{\boldsymbol{p}}} = p_3 \hat{\underline{\boldsymbol{e}}}_3$. At this stage, the microstructure of the plate is not specified.

The membrane stress $N_{\alpha\beta}$, the bending moment $M_{\alpha\beta}$, and shear forces Q_α are the usual generalized stresses for Reissner–Mindlin plates. Both $\underset{\sim}{\boldsymbol{N}}$ and $\underset{\sim}{\boldsymbol{M}}$ follows the symmetry of stress tenors: $N_{\alpha\beta} = N_{\beta\alpha}$ and $M_{\alpha\beta} = M_{\beta\alpha}$. Moreover, we introduce an additional static unknown: the gradient of the bending moment $\underset{\frown}{\boldsymbol{R}} = \underset{\sim}{\boldsymbol{M}} \otimes \underline{\boldsymbol{\nabla}} = M_{\alpha\beta,\gamma}$. The 2D third-order tensor $\underset{\frown}{\boldsymbol{R}}$ complies with the following symmetry: $R_{\alpha\beta\gamma} = R_{\beta\alpha\gamma}$. It is possible to derive shear forces $\underline{\boldsymbol{Q}}$ from $\underset{\frown}{\boldsymbol{R}}$ with: $\underline{\boldsymbol{Q}} = \underset{\approx}{\boldsymbol{i}} \therefore \underset{\frown}{\boldsymbol{R}} \iff Q_\alpha = R_{\alpha\beta\beta}$. Here $\underset{\approx}{\boldsymbol{i}}$ is the identity for in-plane elasticity: $i_{\alpha\beta\gamma\delta} = \frac{1}{2}\left(\delta_{\alpha\gamma}\delta_{\beta\delta} + \delta_{\alpha\delta}\delta_{\beta\gamma}\right)$, where $\delta_{\alpha\beta}$ is Kronecker symbol ($\delta_{\alpha\beta} = 1$ if $\alpha = \beta$, $\delta_{\alpha\beta} = 0$ otherwise). The full bending gradient $\underset{\frown}{\boldsymbol{R}}$ has six components whereas $\underline{\boldsymbol{Q}}$ has two components. Thus, using the full bending gradient as static unknown introduces four additional static unknowns. More precisely: R_{111} and R_{222} are respectively the cylindrical bending part of shear forces Q_1 and Q_2, R_{121} and R_{122} are respectively the torsion part of these shear forces and R_{112} and R_{221} are linked to strictly self-equilibrated stresses.

The main difference between Reissner–Mindlin and Bending-Gradient plate theories is that the Bending-Gradient plate theory enables the distinction between each component of the gradient of the bending moment whereas they are mixed into the shear forces with Reissner–Mindlin theory. In the case of highly anisotropic laminated plates this distinction is critical for deriving good estimate of the deflection and local transverse shear distribution through the thickness (Lebée and Sab, 2011b).